Geothermal Convection and Double Diffusion Based on Profiling Floats in the Black Sea

E. V. Stanev[1,2,3] , **B. Chtirkova[2,3,4]** , and **E. Peneva[3]**

[1]Institute of Coastal Research, Geesthacht, Germany, [2]Research Department, Sofia University "St. Kliment Ohridski", Sofia, Bulgaria, [3]Department of Meteorology and Geophysics, Faculty of Physics, Sofia University "St. Kliment Ohridski", Sofia, Bulgaria, [4]Institute for Atmospheric and Climate Science, Zurich, Switzerland

Abstract Here, we revisit the existing concepts of the vertical structure of deep layers in the Black Sea using data from sensors deployed on profiling floats. The deep transition layer (DTL) between 700 and 1,700 m acts as an interface between the baroclinic layer and the largest bottom convective layer (BCL) of the world oceans. On top of DTL are the warm intermediate layer and deep cold intermediate layer. They both showed strong trends in the last 15 years due to warmer climate and intensification of warmer intrusions from Bosporus. A "salinity wave" was detected in 2005–2009 below ~1,700 m, which evidenced for the first time the penetration of gravity flow from Bosporus down to the bottom. The layering of water masses was explained as resulting from the different distribution of sources of heat and salt, double diffusion, and balances between the geothermal and salinity flows in the BCL.

Plain Language Summary A total of 5,927 profiles from 31 profiling floats deployed in the Black Sea after 2005 were used to study the thermohaline dynamic. The density ratio, which sets the conditions under which double diffusion could occur qualifies most of the depths below 600 m as a double-diffusive environment, which was confirmed by the observed staircase structure of vertical profiles. The qualitative differences between the temperature and salinity profiles in DTL are explained by the different distributions of sources and sinks of heat and salt. This layer acts as a transition zone between the bottom convective layer and the baroclinic ocean. A deep cold intermediate layer (DCIL) occupies the top of the DTL. The former became pronounced in recent years as a consequence of the warming of upper water layers. The large salinity variations from 2005 to 2009 observed at the bottom of the DTL evidenced traces of the penetration of the Bosporus plume down to the bottom for the first time. Combining known values of geothermal flow and concepts from the theory of dynamics of salinity-stratified tanks heated from below made it possible to quantify the mean annual volume of Bosporus water reaching the bottom.

1. Introduction

It is a common knowledge that air-sea exchange, river runoff, and astronomical forces provide the major driving forces for the world ocean. The role of geothermal flows, which are much smaller than heat flows at the ocean surface, remains largely unknown. There are, however, ocean basins, which can be considered excellent natural laboratories for studying the impact of geothermal flows on ocean dynamics. The Black Sea provides one such natural laboratory. It is one of the best places to observe the large-scale effects of bottom convection and double diffusion, as well as to develop concepts and methods, which can be transferred to other similar ocean areas.

The Black Sea bottom convective layer (BCL), which is located between a depth of ~1,700 m and the bottom, was first discovered by J. W. Murray et al. (1991). With a thickness of ~400 m in the deepest parts of the sea, it is the largest known convective layer in the world's ocean spreading across the entire basin (Kelley et al., 2003; Radko, 2013). Convection is maintained by a geothermal heat flux of ~0.040 W/m^2 (Duchkov & Kazantscv, 1988; Erickson & Simmons, 1974; Zolotarev et al., 1979) and tends to destabilize otherwise stable salinity stratification (Ozsoy & Besiktepe, 1995; Ozsoy et al., 1993). To date, the temporal and spatial dynamics in deep layers of the Black Sea are not fully understood, nor is the overall significance of double diffusion for the thermohaline state of this basin.

In stable stratified fluids, a double-diffusive regime could form because the molecular diffusivity of temperature $k_T = 1.4 \cdot 10^{-7}$ m^2 s^{-1} is 2 orders of magnitude larger than that for salt $ks = 1.1 \cdot 10^{-9}$ m^2 s^{-1} (Radko, 2013; Stern, 1960). In the Black Sea, as in the Arctic, double diffusion is a result of the competition between a destabilizing temperature gradient and a stable salinity gradient; hence, thermal stratification provides the energy source for diffusive convection. This situation occurs in laboratory experiments when a salinity-stratified tank is heated from below (Turner, 1965, 1968). In most of the water column of the Black Sea, the density ratio, which is defined as $R_\rho = \dfrac{\dfrac{\beta dS}{dz}}{\dfrac{\alpha d\theta}{d}}$, ranges from ~0.5 to infinity. Here θ and S are the potential temperature and salinity, respectively, and α and β are the coefficients of thermal expansion and salinity contraction. Double diffusion, which is known to occur in this range, is most likely the main vertical transport mechanism for heat and salt in the Black Sea pycnocline and below it (J. W. Murray et al., 1991; Ozsoy et al., 1991). Because it is still not possible to clearly identify the depth ranges where double diffusion occurs, we will refer to the layer between 700 and 1,700 m as the deep transition layer (DTL, more justification of this name will be given later). As explained in these works and by Ruddick and Richards (2003), a number of mechanisms, such as gravity current dynamics and associated entrainment, trigger interleaving and set the depth reached by the Bosporus plume. The mixing between coastal and open ocean waters is evidenced by thermohaline intrusions in strong fronts, thus interleaving bridges mesoscale stirring and molecular dissipation.

Over the past 15 years, profiling floats have provided a considerable amount of data and proved to be a powerful instrument to detect the intrusive properties of Black Sea water masses (A. Falina et al., 2007; Stanev et al., 2017, 2018). However, those data were analyzed mainly in the upper layers of the sea. In the present study, we revisit the composition and evolution of thermohaline properties in the deep part of the Black Sea based on data from profiling floats. The major objective of this study is to further clarify the existing concepts and provide new interpretations of the structure of water masses and processes below the main pycnocline. We focus on the formation mechanisms of deep-water masses, which are still not very clear, as well as on the corresponding temporal and spatial evolution patterns, including recent trends. Of fundamental interest are the dynamics of DTL playing the role of a thick interface between the pycnocline and BCL. New findings about deep-ocean ventilation are also presented.

2. Materials and Methods

2.1. A Description of Observations

Profiling floats deployed after 2005 (Akpinar et al., 2017; Grayek et al., 2015; Korotaev et al., 2006; Stanev et al., 2013, 2019) provide almost uniform coverage of the Black Sea area (Figure 1a). Here, we use data from 31 floats, or 5,927 profiles in total. Most data are from the upper 900 m of the water column; however, their amount down to 1,500 m is large (see the inset in Figure 1a) compared to those from earlier studies. Three of the floats collect data down to 2,000 m, which is approximately the maximum basin depth. Notably, 52 profiles in the BCL were available for the analysis (the black symbols in Figure 1a). Technical information and methodological details such as parking depths, locations, vertical sampling depths, float types, and sensor characteristics are given in the supporting information and in the above-cited publications.

Two floats collected data every 1 m from 200 to 1,000 dbar. Figure 1b demonstrates how the extremely small vertical temperature gradient of ~0.02°C/100 m in the DTL is resolved with a sampling rate of 1 db and sensor accuracy of 0.001°C. The regularly distributed "stairs" reveal a discrete linear increase in temperature, as seen by the observational setup. Five recorded values with equal temperatures are followed by a jump to a temperature that is 0.001°C higher. Obviously, the accuracy of the temperature sensor is the limiting factor, and depth oversampling can occur. The observed temperature stairs thicker than 10 m demonstrate that profiling floats can detect traces of double diffusion below the pycnocline. The capabilities of individual floats to detect the "stairs" as dependent on the vertical sampling rate is shown in Figure S1.

One example of how a deep float observes the variability in temperature and salinity below 400 m is shown in Figures 1c and 1d. While salinity is a monotonously increasing function of depth, θ displays several
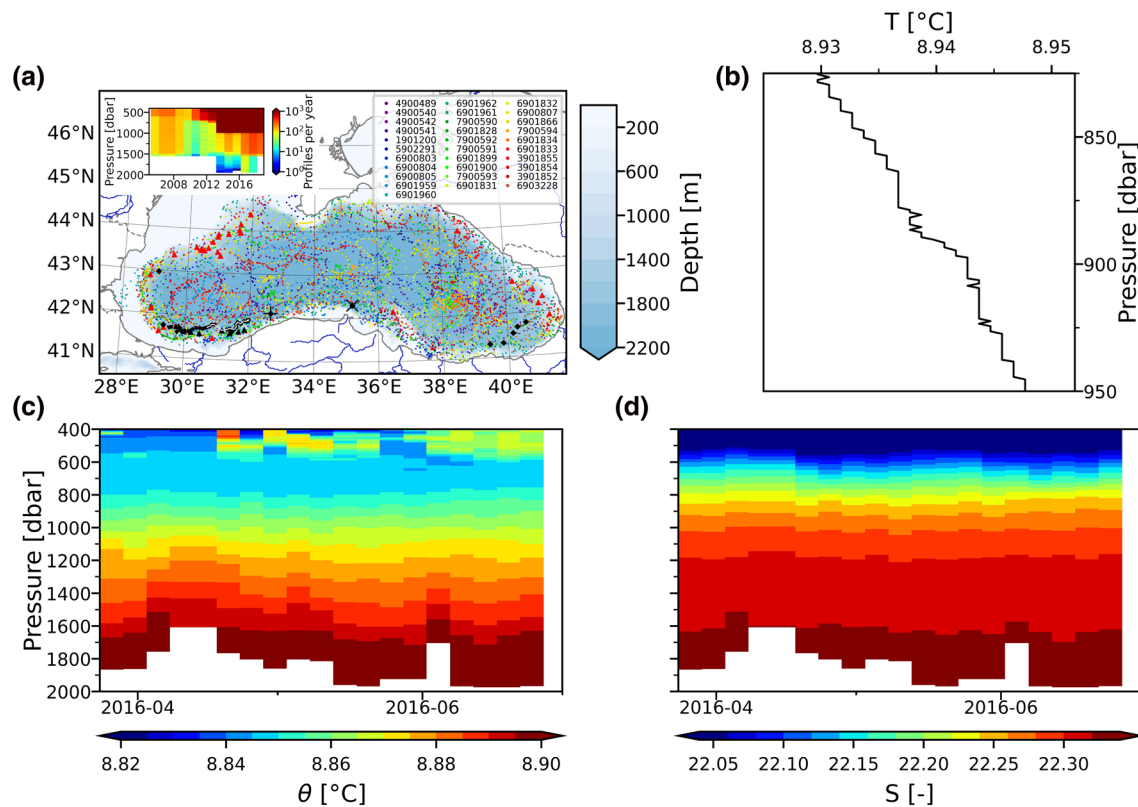
Figure 1. (a) Argo sampling positions from March 2005 to March 2020. Different colors correspond to individual floats (see the identification numbers in the legend inset in the top right corner). The inset in the top left corner shows the number of profiles per year as a function of depth. The light blue background colors show the depths. Red triangle symbols denote the positions of warm intrusions below 900 m that are to the right of the blue line in Figure 2b. (b) The in situ temperature, as measured by float 7900591 on 2016-01-11. (c and d) Examples of time versus depth diagrams from the deep profiling float 7900594 below 400 m. Its trajectory for the period shown in (b, c) is plotted with the white line. Black diamond, triangle, and circle symbols denote the float measurements deeper than 1,600 m obtained by floats 7900590, 7900593, and 7900594, respectively. The large "+" and "x" symbols overlying the "standard" (diamond) symbol in (a) show the positions where the BCL was (almost) not observed in the profiles on January 28 and March 19, 2014, respectively.

warm intrusions at ~500 m due to a mixture of warm Marmara Sea water and ambient water (A. Falina et al., 2007; Ozsoy, et al., 1993). Below these intrusive depths is a layer at ~700 m with low temperatures (herein called the deep cold intermediate layer, DCIL). Below DCIL, θ increases with increasing depth. In a number of locations, the temperature shows higher or lower temperatures below 1,200 m, illustrating that the properties at these depths are far from horizontally uniform. These changes are recorded down to ~1,600 m, which is close to the upper boundary of the BCL.

3. Vertical Structure of Water Masses

The enlarged presentation of the vertical structure of water masses in Figure 2 is used to show the specific variability ranges in the entire water column (left panels), lower part of the main pycnocline and DTL (panels in the middle), and BCL (panels on the left). With the large number of available profiles, credible statistics can be obtained; therefore, the data are presented as probability distributions of the respective properties, illustrating the corresponding spreads in individual layers (bins). Because the number of profiles in the BCL is relatively low for obtaining results with statistical credibility, the individual profiles are shown in the panels on the right-hand side.

The cold intermediate layer (CIL) is identified by the minimum temperature core at the top of the permanent halocline (Figure 2a). At the top of the DTL, at ~700 m, the vertical gradient of θ strongly decreases (Figure 2b), and the DCIL appears as a very clear feature in the vertical temperature distribution. This layer
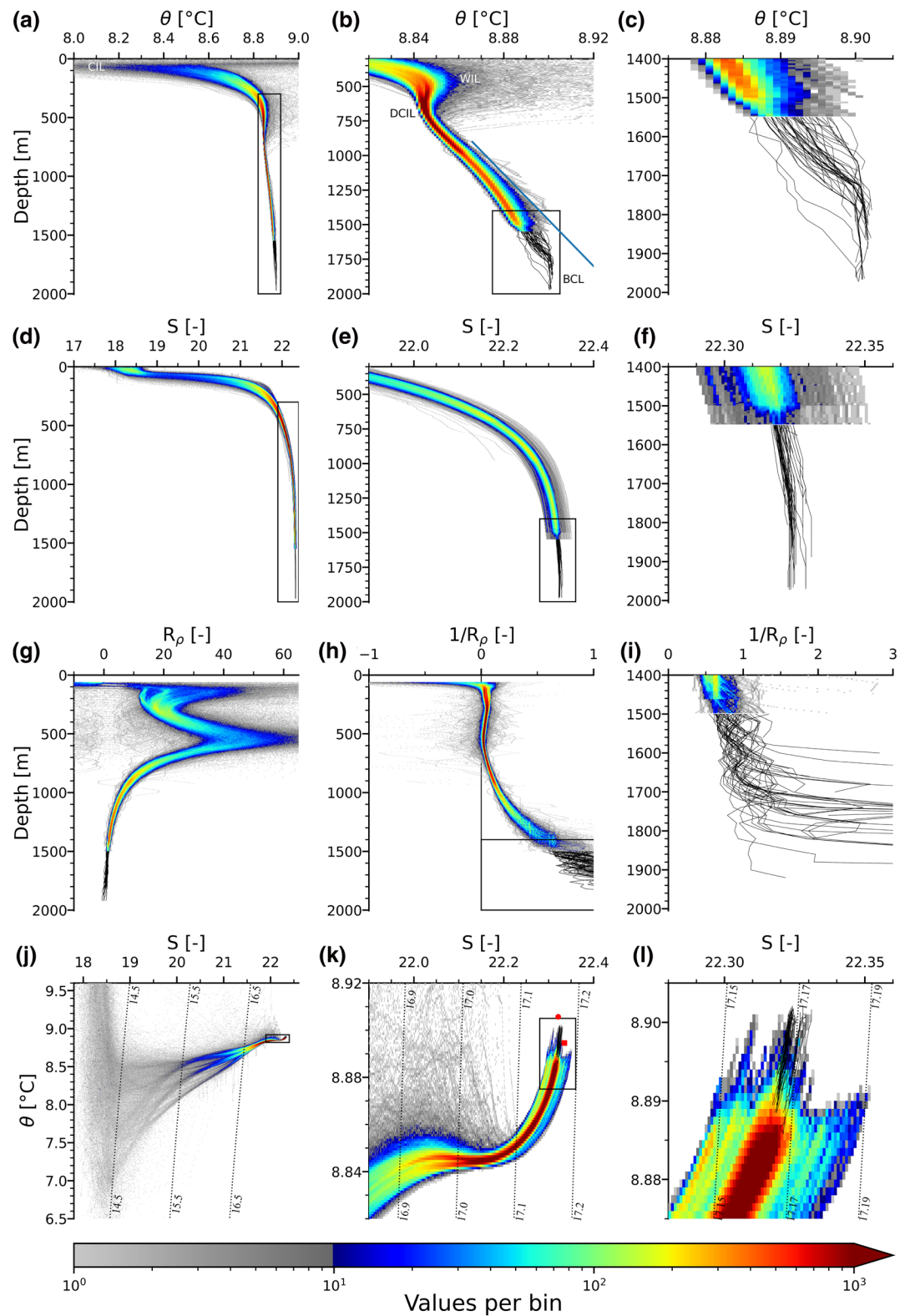
is similar to the CIL in the sense that the vertical gradients of θ are near zero in both cases. J. W. Murray et al. (1991) were the first to discover a DCIL; however, it has not been well addressed in the literature, nor have its dynamics and persistence.

Figure 2b reveals a warm intermediate layer (WIL) with a core at ~541 ± 60 m. Positive temperature anomalies at these depths have also been documented by J. W. Murray et al. (1991) and A. S. Falina and Volkov (2004); however, they have not received much consideration. The "pair" WIL-DCIL in Figure 2b shows a fundamental transition of Black Sea physics at the bottom of the pycnocline. The positive temperature anomalies above the dominant mixing curves in the main pycnocline (Figures 2b and 2k) illustrate the intrusions of warm waters from the Bosporus down to $\sigma_\theta = 17.1$. While the WIL is clearly related to deep intrusions (warm waters of Bosporus origin "pull" the temperature profiles toward higher values), the origin of the DCIL is not so clear because no cold intrusions are seen in Figure 2k. What has not been documented before is the spread of data below 750 m seen as positive temperature anomalies (to the right of the blue line in Figure 2b). Their positions marked by the red triangular symbols in Figure 1a suggest enhanced deep water mixing on the continental slope.

The accuracy of sampling does not allow us to sufficiently resolve the double-diffusive instability, which operates on centimeter scales. Therefore, the focus is placed on the macroscale features associated with double diffusion. $R\rho$ gives a robust estimate of the possibility of double diffusion. At ~550 m (WIL), $R\rho$ > 60 (Figure 2g) and becomes very small below 1,500 m. Because of the very small values, $1/R\rho$ profiles are also presented in Figures 2h and 2i. Obviously, the diffusive regime of instability $1 < R\rho < 10$ (Radko, 2013) is characteristic for most depths below 800 m (see staircases in Figure 1b). Staircases at shallower depths (Figure S1) suggest that either double diffusion could occur for larger $R\rho$ values (this would confirm a similar statement of Radko, 2013), or those are traces of intrusions in the WIL. There are also many individual profiles up to the DCIL for which $R\rho < 10$, that is, double diffusion could also occur there.

Below the core of the DCIL and down to the upper boundary of the BCL at ~1,750 m, θ increases almost linearly (Figure 2b, see individual profiles in Figure S1). However, the increase in S over the same depth interval is clearly nonlinear (Figure 2e). Therefore, $1/R\rho$ increases nonlinearly (Figure 2h). The deep-ocean θ-S curves reverse curvature at depths between the WIL and DCIL (Figure 2k). The almost linear θ-S relationships in the pycnocline (Figure S2) transform into curved profiles (a similar individual profile was shown by J. W. Murray et al., 1991), demonstrating the dominant role of diapycnal mixing in the DTL (see also Schmitt, 1981).

At the base of the DTL, θ-S curves asymptotically approach density lines, which means that at these depths, the contributions of temperature, and salinity to the density are approximately equal. The DTL can be considered a thick (~1,000 m) water body in which θ-S lines change direction from almost normal to isopycnal (in the halocline) to tangential (in the BCL). Vertical profiles of θ show a vertically uniform distribution in the BCL (panels on the right, see also Figure S1). The kink at ~1,700 m identifies the top of the BCL; its depth ranges ~150 m (Figure S1). The increasing values of $1/R\rho$ up to ~3 (Figure 2i) reflect the predominance of temperature (Figure 2c). Notably, values of ~2.6 have been reported for the upper boundary of the BCL by V. N. Eremeev et al. (1998).

Two profiles from float 7900590 taken on January 28 and March 19, 2014 (the left most profiles in Figure 2c, see also Figure S1) demonstrate extremely deep positions of the top of the BCL, below 1,840 and 1,940 m, respectively. Many profiles do not show BCL at all (Figures 2c and S1). Furthermore, the warming from the shallower bottom tends to penetrate higher in the DTL (Figure 1c). Obviously, the BCL is not stationary, nor is it spatially uniform. Its upper boundary is not horizontal, which can be due to spatial changes in geothermal flow (Starostenko et al., 2014).

Figure 2. Thermohaline properties in the Black Sea: (a–c) potential temperature; (d–f) salinity; (g–i) density ratio; (j–l) θ-S diagrams. The panels on the left show the properties for the entire water column; those in the middle are enlarged presentations below 400 m; the panels on the right are zoomed plots for the BCL region (below 1,400 m). The ranges of these zoomed plots are shown in the respective panels on the left (boxes). Additionally, the inverse density number is shown in (h and i). Data are presented as probability distributions (the number of data points in the individual coordinate bins). Because fewer observations were obtained below 1,500 m, the individual profiles are shown with black lines. Temperatures lower than 8°C and higher than 9°C in the surface layer are excluded in (a) to provide a high-resolution plot of the deep layers. For the same reasons, temperatures higher than 9.6°C and lower than 6.5°C are excluded in (j). The blue line in (b) is used to distinguish the warm intrusions below 900 m, which are plotted as red triangles in Figure 1a. The red circle and square symbols in (k) show the observed by J. W. Murray et al. (1991) θ = 8.9057°C and S = 22.3212 in the BCL and the respective mean values of θ and S from the Knorr 2001, 2003, and Endeavor 2005 cruises (J. W. Murray et al., 2005; http://www.ocean.washington.edu/cruises/Endeavor2005).

Comparisons with the CTD observations during the cruises of R/V Knorr in 2001 and 2003 and R/V Endeavor in 2005 (J. W. Murray et al., 2005; http://www.ocean.washington.edu/cruises/Endeavor2005) reveal a very similar hydrological structure (Figure S3). The CTD profiles at 800 m are ∼0.005°C colder than the coldest profiles from the floats, illustrating a recent warming below the baroclinic layer (compare also the observations in Figure 2b and Figure S2b with respect to the position of blue line). The WIL-DCIL pair was less pronounced at the beginning of 2000s. Notably, there are two CTD profiles down to 2,000 m where BCL does not occur, similar to the case with the profiling floats described above.

4. Temporal and Spatial Variability

The time versus depth diagrams in Figure 3 show all the profiles below 400 m, each of which appears chronologically. This presentation is meaningful because the spatial and temporal variability at these depths is small. The major finding is that after 2013, the DCIL with a core at ∼700 m became a persistent thermohaline feature; in the first part of the observation period, waters at this depth were only intermittently overlain by warm intrusions (compare also profiles in Figure S2b with much older profiles in Figure S3b). Therefore, the WIL and DCIL can be regarded as variable elements of the vertical stratification. Their appearance over the past 15 years parallels the continuous increase in $R\rho$ (Figure 3c).

Below 1,000 m, the temperature variations are characterized by warm anomalies originating from deeper depths (Figure 1c). Four floats that operated almost simultaneously from 2005 to 2009 registered a "salinity wave," with a minimum in 2007 (Figure 3b). They were deployed northeast of the Bosporus Strait as tandems of two floats per release. The short distance from the strait (see Figure S4 for their trajectories) would explain the high salinity values at the release positions. However, many other floats sampled this region (Figure 1a) and never registered values as high as those of these four floats. Moreover, after a year of operation, salinity reached a minimum, and a continuous increase then occurred until the present salinity levels were reached. Notably, these high-amplitude oscillations were detected not only in the near-Bosporus area but also in the eastern basin. This "salinity wave" could be due to salinity intrusions deeper than 1,500 m resulting in a doubling of the salinity range in 2005–2009 compared to the rest of the period of observations.

There is a persistent increase in temperature in the WIL after 2014 (Figure 3a), illustrating that the changes in the Bosporus intrusions parallel the recent warming in the upper Black Sea (Stanev et al., 2019; Stanev & Chtirkova, 2021). It seems thus very plausible that the temperature of the inflowing water may have also increased in the past decade because of the warming trends in the Mediterranean. The comparison of the data in 2000s with those of the R/V Knorr cruise in 1988 (J. W. Murray et al., 1991), the latter of which is depicted by the red circle symbol in Figures 2k and S3k, shows that salinity remained almost the same, but θ decreased by ∼0.005°C.

5. Discussion

5.1. Heat and Salt Balances

Most intrusions occur down to 600–700 m, which is in agreement with the observations of Ozsoy et al. (1993) and modeling results of Stanev et al. (2004). However, the "salinity wave" detected below ∼1,700 m supports the statement of J. W. Murray et al. (2006) that "occasional or rare ventilation events" can reach the bottom. As demonstrated by V. N. Eremeev et al. (1997, 1998), a salinity flux into the BCL needs to be postulated to adequately represent the thermohaline structure of deep Black Sea waters. Without a salt flux, convection due to geothermal heat flow causes the upper boundary of the BCL to continuously ascend. Adding a negative haline buoyancy flux $B_{salt} = g\beta Q_W S$, which opposes the positive heat buoyancy flux $B_{heat} = -g\alpha Q_T/(\rho_0 c_W)$, would prevent this. In other words, the potential energy released by the temperature field (or fraction m of it) is used to lift the salt (Turner, 1965). Here, geothermal flow Q_T and water flow caused by the bottom plumes that reached the bottom Q_W have units of [W/m^2] and [m/s], respectively. From $SQ_W = m\alpha Q_T/(\beta\rho_0 c_W)$, it follows that a value of $Q_T = 0.04$ W/m^2 would correspond to $Q_W \sim 10^{-10}$ m/s, or the annual addition of ∼1 km^3 water in the BCL (area is taken as 4×10^6 km^2 and $m = 1$). This volume is ∼1/300 of the inflow through the Bosporus Strait. If $m = 0.15$, as in the experiments of Turner (1965), the needed annual volume of water from Bosporus origin is 0.15 km^3.
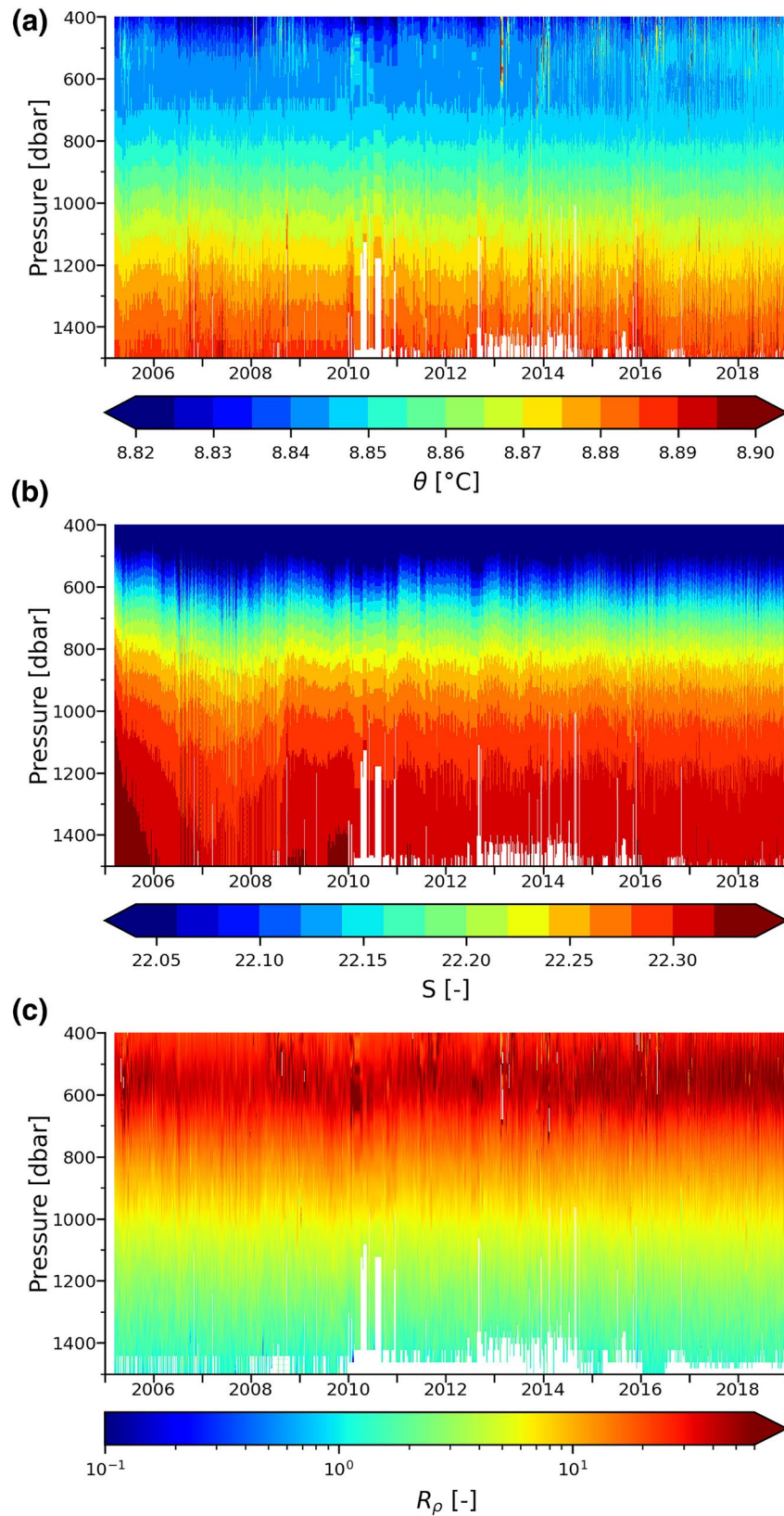
Figure 3. Time versus depth diagrams of (a) potential temperature, (b) salinity, and (c) $R\rho$ between 400 and 1,500 m. The vertical markers of the *x*-axes correspond to 1 January each year. White areas indicate no data (not sampled or shallow depths) or bad data.

How does the heat flux from the gravity flow that reached the bottom compare against Q_T? Knowing that $\beta/\alpha > 5$ and taking for salinity and temperature differences between Marmara Sea and Black Sea waters $\Delta S = 18$ psu and $\Delta T = 3°C$, it follows that $R_\rho{}^{Bo} = \beta\Delta S/\alpha\Delta T > 30$. This number reflects the small available potential energy stored initially in the temperature (unstable component). Knowing that gravity flow mixes temperature and salt at the same rate, it follows that $Q_T{}^{Bo}/Q_T < 30$ (if $m = 1$). One can thus conclude that the warming of the BCL by gravity flow is negligible compared to that by geothermal flow. Therefore, to the statement of J. W. Murray et al. (2006) "the only source of salt (and warm) water is through the Bosporus, and the only source of cold (and fresh) water is from the surface," one needs to add geothermal flow, which is fundamental for the properties of Black Sea water in the DTL and BCL. Notably, this flow is 5 times smaller than the heat flux through the Arctic staircases reported by Timmermans et al. (2008) but is comparable to the estimates of Padman and Dillon (1987). Here, we remember that the Arctic Ocean, like the Black Sea, is predominantly stratified by salinity.

5.2. Vertical Stratification Above the DCIL

Starting from the sea surface, the first element of vertical stratification is the mixed surface layer. The baroclinic layer, where the gravity currents from Bosporus and dynamics of the front trigger isopycnal mixing, extends to depths of ∼600 m. Considering that diapycnal turbulent mixing is proportional to the curvature of the θ-S line (McDougall, 1984) and taking into consideration the curvature of the θ-S diagrams in CIL (Figure 2j) and DTL (Figure 2k), one can conclude that those are layers where diapycnal mixing plays a substantial role. CIL and DCIL can be considered the natural upper and lower boundaries of the baroclinic layer. Between them, from $\sigma_\theta \sim 15.8$ kgm^{-3} to $\sigma_\theta \sim 16.8$ kgm^{-3}, we observe straight θ-S lines (see also Figure S2), demonstrating that in most cases, temperature and salinity mix at equal rates (presumably due to fully developed turbulent diffusion and entrainment). Stanev and Chtirkova (2021) explained the different slopes of linear segments of the θ-S relationship as being due to several extreme cooling events and warming climates in the last 15 years.

J. W. Murray et al. (1991) and Ozsoy et al. (1991) reported cold water intrusions down to 600 m and explained them as being due to mixing of water from the Bosporus and water from the CIL. In the past 15 years, warm winters have resulted in a substantial reduction in the cold water volume and oxygen content in the CIL (Capet et al., 2016; Stanev et al., 2019). Cold water intrusions were rare, but warm intrusions became dominant. One can thus explain the origin of the WIL and DCIL as resulting from the variability of the properties of waters originating from Bosporus and the warming of the CIL. One simple scenario would suggest that the vertical temperature profiles above ∼600 m move back and forth (compare Figures 2b and S3b), reducing the temperatures of the WIL in the cold phases and warming it in the warm phases. Thus, the WIL and DCIL pair cannot be considered in isolation from each other. The DCIL, like the CIL, is a variable end member that strongly responds to climate change and resulting in changes in the upper ocean. Recent climatic changes have made the WIL-DCIL pair more distinguishable than in the past.

There were no cold intrusions at 750 m recorded by profiling floats during the last 15 years, which justifies the following two questions. (1) Is the DCIL a relict water mass or is it intermittently refilled by cold water intrusions? (2) How low the turbulence has to be to avoid destroying the DCIL? Taking for the thickness of DCIL 100 m and using for the coefficient of vertical diffusion the "canonical" value $K = 10^{-5}$ m^2 s^{-1} yields a characteristic time T_{DCIL} of ∼30 years. This time would be much longer if $K << 10^{-5}$ m^2 s^{-1}, which could be the case in the nontidal Black Sea (M. Gregg & Ozsoy, 1999; M. C. Gregg & Yakushev, 2005). Approximately 30 years have passed since J. W. Murray et al. (1991) showed that there is a temperature minimum at ∼600 m. This minimum was ∼0.005°C cooler and ∼100 deeper than the minimum in Figure 2b (we remember that J. W. Murray et al., 1991 showed only one profile). Without continuity of observations over at least several decades, the answer to question (1) is still unknown. As far as the answer to question (2) is concerned, it cannot be excluded that low turbulent diffusion at the bottom of the pycnocline contributes to the persistence of DCILs.

5.3. Vertical Stratification Below the DCIL

The temperature below the DCIL shows a linear profile, while the salinity profile is curved (Figures 2b and 2e). This is reflected in the curved θ-S distribution in DTL. These different θ and S profiles are due to differ-

ent distributions of sources and sinks. For temperature, we assume that there are no sinks between the top of the BCL and DCIL. If $K = 10^{-4}$ m^{2}s^{-1} in the rather homogenous layers below the pycnocline and $Q_T = 0.04$ W/m^2, the slope of the linear θ-profile equals that in the observations. Obviously, the geothermal flows impact not only the BCL (up to 1,700 m) but also the θ profile in the transition layer between the BCL and the baroclinic ocean. As shown by Stanev et al. (2004), a realistic salinity profile can be reproduced in a 1-D model depending on the ratio between entrainment and detrainment; that is, the curved profile of salinity is due to the dynamics of gravity flow in the DTL. The different distribution of sources of heat and salt (salt originates only from Bosporus, heat has a source at the bottom) explains the differences in the respective θ and S profiles and the specific shape of $R\rho$, the latter sets the conditions for existence of double diffusion above the BCL and in most of the water column up to the DCIL.

6. Conclusions

The CIL and DCIL appear to be the natural upper and lower boundaries of the baroclinic layer. Below DCIL is the DTL, where the θ-S lines change direction from almost normal to isopycnal (in the halocline) to tangential (in the BCL). Therefore, the DTL acts as a transition layer between the baroclinic ocean, which is dominated by isopycnal mixing maintained by frontal dynamics and intrusions of waters of Bosporus origin, and the BCL. In this transition layer, the vertical profiles of temperature and salinity largely differ because of the different distributions of their sources and sinks.

In the 1990s, a number of deep and cold temperature intrusions were observed, but they have rarely appeared in recent years. After 2013, the WIL-DCIL became a persistent thermohaline feature due to the warming of the waters from the Bosporus and waters in the CIL. DCILs can be regarded as a variable thermohaline end member that responds to changes in the upper layers and properties of gravity currents.

Four profiling floats registered a "salinity wave" at the base of the DTL. It is not plausible that the four floats were all malfunctioning, which suggests that we discovered very deep salinity intrusions not previously reported. This finding provides observational support for the concept that such a flow must exist to close physical balances controlling the thermohaline state of deep layers. The concept developed here that deep water variability caused by the interaction between the upper ocean and deep sea through gravity flows presents a generalization of earlier concepts, according to which the temporal variability of Black Sea water masses occurs in the layers above the permanent pycnocline.

BCL is not homogenous and stationary, as previously claimed. Its upper boundary reveals large spatial-temporal variability. Temperature anomalies from the BCL can be traced in the DTL up to at least 1,400 m, particularly over the shallower bottom. We hope that our results could motivate similar studies in other inland ocean basins or world oceans (remember the similarity between double diffusion in the Black Sea and in high latitudes, Ruddick and Richards, 2003; Kelley et al., 2003), as well as numerical modeling, which could test various scenarios about the role of geothermal flows and double diffusion in ocean dynamics.

Data Availability Statement

The data used in this study are available at ftp://ftp.ifremer.fr/ifremer/argo/dac/coriolis/, http://marine.copernicus.eu/.

References

Akpinar, A., Fach, B. A., & Oguz, T. (2017). Observing the subsurface thermal signature of the Black Sea cold intermediate layer with Argo profiling floats. *Deep Sea Research Part I: Oceanographic Research Papers*, *124*, 140–152. https://doi.org/10.1016/j.dsr.2017.04.002

Capet, A., Stanev, E. V., Beckers, J.-M., Murray, J., & Gregoire, M. (2016). Decline of the Black Sea oxygen inventory. *Biogeosciences*, *13*(4), 1287–1297. https://doi.org/10.5194/bg-13-1287-2016

Duchkov, A. D., & Kazantscv, S. A. (1988). *Thermal flux ill the Black Sea trough Geophysical Fields of the Atlantic Ocean*. Moscow, Russia: Nauka, 121–130.

Eremeev, V. N., Ivanov, L. I., Samodurov, A. S., & Duman, M. (1997). The Black Sea bottom homogeneous layer: A simple model of formation. In E. Özsoy & A. Mikaelyan (Eds.), *Sensitivity to change: Black Sea, Baltic Sea and North Sea. NATO ASI Series (Series 2: Environment)* (Vol. 27, pp. 275–283). Dordrecht, The Netherlands: Springer.

Eremeev, V. N., Ivanov, L., Samodurov, A. S., & Duman, M. (1998). The near-bottom boundary layer in the Black Sea: Hydrological structure and modelling. *Physical Oceanography*, *9*(2), 79–101. https://doi.org/10.1007/BF02525515

Erickson, A., & Simmons, G. (1974). Environmental and geophysical interpretation of heat flow measurements in Black Sea. In E. T. Owens & D. A. Ross (Eds.), The Black Sea-geology, chemistry and biology (Vol. 20, pp. 50–62). American Association of Petroleum Geologists, Memoir.

Falina, A., Sarafanov, A., & Volkov, I. (2007). Warm intrusions in the intermediate layer (150-500 m) of the Black Sea eastern gyre interior. *Geophysical Research Letters*, *34*, L22602. https://doi.org/10.1029/2007GL031016

Falina, A. S., & Volkov, I. I. (2004). Influence of double diffusion on general thermohaline structure of the Black Sea deep waters. *Okeanologya*, *44*(6), 1–11.

Grayek, S., Stanev, E., & Schulz-Stellenfleth, J. (2015). Assessment of the Black Sea observing system. A focus on 2005-2012 Argo campaigns. *Ocean Dynamics*, 1–20. https://doi.org/10.1007/s10236-015-0889-8

Gregg, M., & Ozsoy, E. (1999). Mixing on the Black Sea shelf north of the Bosporus. *Geophysical Research Letters*, *26*, 1809–1872.

Gregg, M. C., & Yakushev, E. (2005). Surface ventilation of the Black Sea's cold intermediate layer in the middle of the western gyre. *Geophysical Research Letters*, *32*, L03604. https://doi.org/10.1029/2004GL021580

Kelley, D. E., Fernando, H. J. S., Gargett, A. E., Tanny, J., & Ozsoy, E. (2003). The diffusive regime of double-diffusive convection. *Progress in Oceanography*, *56*, 461–481.

Korotaev, G., Oğuz, T., & Riser, S. (2006). Intermediate and deep currents of the Black Sea obtained from autonomous profiling floats. *Deep Sea Research Part II: Topical Studies in Oceanography*, *53*(17–19), 1901–1910. https://doi.org/10.1016/j.dsr2.2006.04.017

McDougall, T. J. (1984). The relative roles of diapycnal and isopycnal mixing on subsurface water mass conversion. *Journal of Physical Oceanography*, *14*, 1577–1589.

Murray, J. W., Fuchsman, C., Kirkpatrick, J., Paul, B., & Konovalov, S. K. (2005). Species and δ^{15}N signatures of nitrogen transformations in the suboxic zone of the Black Sea. *Oceanography*, *18*(2), 36–47. https://doi.org/10.5670/oceanog.2005.40

Murray, J. W., Stewart, K., Kassakian, S., Krynytzky, M., & DiJulio, D. (2006). Oxic, suboxic and anoxic conditions in the Black Sea. In A. Gilbert, V. Yanko-Hombach, & N. Panin (Eds.), *Climate change and coastline migration as factors in human adaptation to the Circum-PonticRegion: From past to forecast* (pp. 437–452). New York, NY: Kluwer.

Murray, J. W., Top, Z., & Ozsoy, E. (1991). Hydrographic properties and ventilation of the Black Sea. *Deep-Sea Research*, *38*, S663–S689.

Ozsoy, E., & Besiktepe, S. (1995). Sources of double diffusive convection and impacts on mixing in the Black Sea. In A. Brandt & H. J. S. Fernando (Eds.), *Double-diffusive convection, Geophysical Monograph, 94* (pp. 261–274). American Geophysical Union.

Ozsoy, E., Top, Z., White, G., & Murray, J. W. (1991). Double diffusive intrusions, mixing and deep convective processes in the Black Sea. In E. Izdar & J. Murray (Eds.), *Black Sea oceanography. NATO ASI Series C* (Vol. 351, pp. 17–42). Kluwer Academic.

Ozsoy, E., Unluata, U., & Top, Z. (1993). The evolution of Mediterranean water in the Black Sea: Interior mixing and material transport by double diffusive instructions. *Progress in Oceanography*, *31*, 275–320.

Padman, L., & Dillon, T. M. (1987). Vertical heat fluxes through the Beaufort Sea thermohaline staircase. *Journal of Geophysical Research*, *92*, 10799–10806.

Radko, T. (2013). Double-diffusive convection. In *Double-diffusive convection* (pp. 344). Cambridge, UK: Cambridge University Press. ISBN 978-05-218-8074-9

Ruddick, B., & Richards, K. (2003). Oceanic thermohaline intrusions: Observations. *Progress in Oceanography*, *56*(3-4), 499–527. https://doi.org/10.1016/S0079-6611(03)00028-4

Schmitt, R. W. (1981). Form of the temperature-salinity relationship in the Central Water: Evidence for double-diffusive mixing. *Journal of Physical Oceanography*, *11*, 1015–1026.

Stanev, E. V., & Chtirkova, B. (2021). Interannual change in mode waters: Case of the Black Sea. *Journal of Geophysical Research: Oceans*, *125*, e2020JC016429. https://doi.org/10.1029/2020JC016429

Stanev, E. V., Grayek, S., Claustre, H., Schmechtig, C., & Poteau, A. (2017). Water intrusions and particle signatures in the Black Sea: A biogeochemical-argo float investigation. *Ocean Dynamics*, *67*, 1119–1136. https://doi.org/10.1007/s10236-017-1077-9

Stanev, E. V., He, Y., Grayek, S., & Boetius, A. (2013). Oxygen dynamics in the Black Sea as seen by Argo profiling floats. *Geophysical Research Letters*, *40*, 3085–3090. https://doi.org/10.1002/grl.50606

Stanev, E. V., Peneva, E., & Chtirkova, B. (2019). Climate change and regional ocean water mass disappearance: Case of the Black Sea. *Journal of Geophysical Research: Oceans*, *124*, 4803–4819. https://doi.org/10.1029/2019JC015076

Stanev, E. V., Poulain, P.-M., Grayek, S., Johnson, K. S., Claustre, H., & Murray, J. W. (2018). Understanding the dynamics of the oxic-anoxic interface in the Black Sea. *Geophysical Research Letters*, *45*, 864–871. https://doi.org/10.1002/2017GL076206

Stanev, E. V., Staneva, J., Bullister, J. L., & Murray, J. W. (2004). Ventilation of the Black Sea pycnocline. Parameterization of convection, numerical simulations and validations against observed chlorofluorocarbon data. *Deep-Sea Research*, *51/12*, 2137–2169.

Starostenko, V. I., Dolmaz, M. N., Kutas, R. I., Rusakov, O. M., Oksum, E., Hisarli, Z. M., et al. (2014). Thermal structure of the crust in the Black Sea: Comparative analysis of magnetic and heat flow data. *Marine Geophysical Researches*, *35*, 345–359. https://doi.org/10.1007/s11001-014-9224-x

Stern, M. E. (1960). The "salt-fountain" and thermohaline convection. *Tellus*, *12*, 172–175.

Timmermans, M.-L., Toole, J., Krishfield, R., & Winsor, P. (2008). Ice-Tethered Profiler observations of the double-diffusive staircase in the Canada Basin thermohaline. *Journal of Geophysical Research*, *113*, C00A02. https://doi.org/10.1029/2008JC004829

Turner, J. S. (1965). The coupled turbulent transports of salt and heat across a sharp density interface. *International Journal of Heat and Mass Transfer*, *8*(5), 759–760.

Turner, J. S. (1968). The behavior of a stable salinity gradient heated from below. *Journal of Fluid Mechanics*, *33*(1), 183–200.

Zolotarev, V. G., Sochel'nikov, V. V., & Malovitskiy, Y. P. (1979). Results of heat-flow measurements in the Black and Mediterranean Sea basins. *Oceanology*, *19*(6), 701–705.